Supporting Information

Photocrosslinked methacrylated carboxymethyl chitosan/oxidized locust bean gum double network hydrogel for cartilage repair

Can Cheng[a], Xu Peng[a,b], Yihao Luo[a], Shubin Shi[a], Ling Wang[a], Yuhang Wang[a], and Xixun Yu[a]*

a. College of Polymer Science and Engineering, Sichuan University, Chengdu 610065, P.R. China. E-mail: yuxixun@163.com

b. Experimental and Research Animal Institute, Sichuan University, Chengdu 610065, P.R. China.

Pages:15

Experimental methods: 18

Figures: 10

***Xixun Yu (Corresponding author)**

College of Polymer Science and Engineering, Sichuan University,
No.24 South Section 1, Yihuan Road, Chengdu, China, 610065, E-mail: yuxixun@163.com

Materials and methods

Degradation of DCP

The degradation of DCP was performed by exposing the specimens to type II collagenase (50 U/mg). Briefly, initial DCP specimens were weighted and immersed in the collagenase/PBS solution and incubated at 37 ℃ with continuous shaking for a predetermined time (0.5 h, 1 h, 3 h, 6 h, 12 h and 24 h). At each time, the supernatant was collected by centrifugation and the DCP after degradation was washed and lyophilized and weighed again. And the degradation ratio of DCP was calculated as follows:

$$\text{Degradation ratio (\%)} = \frac{W_0 - W_T}{W_0} \times 100\%$$

where W_0 represents the initial weight of DCP before degradation and W_t represents the weight of the corresponding sample after degradation. Data from each sample was calculated using triplicate measurement.

Cytotoxicity of DCP after degradation

The in vitro cytotoxicity of DCP degradation ingredients was assessed by CCK-8 test using L929 fibroblasts. The supernatants of DCP degradation products in different degradation times was added to DMEM medium supplemented with 10% FBS and 1% penicillin-streptomycin. P3 generation L929 fibroblasts were inoculated on 96-well plate at the density of 1×10^4 cells/well and incubated for 24 h to make the cells stick to bottom. Then the original DMEM medium was replaced with fresh medium supplemented with the supernatants of DCP degradation products in different degradation times. The original DMEM medium in control groups was only replaced with fresh medium. At 1 d, 3 d and 5 d, CCK-8 were added to each well and incubated for 1 h in the dark, and then the OD value of solution was measured at 450 nm with a microplate reader. The cell viability was calculated as follows:

$$Relative\ Growth\ Rate\ (\%) = \frac{OD_{sample}}{OD_{control}} \times 100\%$$

Where OD_{sample} and $OD_{control}$ were the optical density of cells in the sample group and the control group respectively. Data from each sample was calculated using triplicate measurement.

Characterization of MA-CMCS and OLBG

The chemical structure of MA-CMCS was characterized by Fourier transform infrared (FTIR) and nuclear magnetic resonance (NMR) spectroscopy. For FTIR measurement, 3 mg dried MA-CMCS and CMCS were mixed with 200 mg potassium bromide (KBr) to press into transparent flake under the pressure of 20 MPa. The FTIR spectra were obtained by Nicolet 560, and the data analysis was performed by OMNIC software. For NMR measurement, D_2O was used to dissolved MA-CMCS and CMCS in NMR tube with a concentration of 10 mg/ml. Hydrogen-1 NMR spectrum analysis was performed by a Bruker Avance II-600 MHz NMR instrument.

The aldehyde group in the chemical structure of OLBG was demonstrated by FTIR. The specific procedure was the same as above.

Crosslinking density of OLBG and MA-CMCS

The crosslinking degree of MA-CMCS and OLBG was assessed using ninhydrin assay. Briefly, 100 μl of MA-CMCS or various hydrogel precursor solutions were added to 2 ml of ninhydrin solution and boiled for 20 min, and the absorbance was measured at 570 nm by a spectrophotometer (UV-752, Shanghai). The crosslinking degree was calculated as follows:

$$Crosslinking\ degree\ (\%) = \frac{NH_{2\ before} - NH_{2\ after}}{NH_{2\ after}} \times 100\%$$

Where $NH_{2\ before}$ is the amount of free amino groups in the MA-CMCS solution, and $NH_{2\ after}$ is the amount of free amino groups in the various hydrogel precursor solutions. Data from each specimen was calculated using triplicate measurement.

Injectability of hydrogels

The hydrogel precursor solution was loaded into a syringe after thorough mixing and injected onto a surgical spreader towel. The precursor solution was photocrosslinked after injection to obtain a phorocurred hydrogel to verify its injectability.

Swelling behavior

The freeze-dried MCOAC hydrogels with loading different concentrations of decellularized cartilage powder (DCP) were processed into similar shapes. The hydrogels were immersed in phosphate buffered saline (PBS) after being weighted, then they were taken out at different times. The moisture on the surface of hydrogel-samples was absorbed with filter paper, they were subsequently weighted again. The swelling

ratio of the hydrogel was calculated as follows:

$$Swelling\ ratio\ (\%) = \frac{m_t - m_0}{m_0} \times 100\%$$

Where m_t is the weight of the hydrogel after swelling at different times, and m_0 is the initial weight of the hydrogel. Data from each specimen was calculated using triplicate measurement.

Water evaporation ratio

The MCOAC hydrogels with different concentrations of DCP were soaked in PBS until the swelling equilibrium was reached. Subsequently, these hydrogel specimens were weighted after using filter paper remove excess water from the surface and recorded as m_1. All these specimens were placed in a constant humidity environment and weighted and recorded as m_2 at different time points (). Finally, the hydrogels were completely dried and reached the constant weight and recorded as m_3. The water evaporation ratio of the hydrogel was calculated as follows:

$$Water\ evaporation\ ratio\ (\%) = \frac{m_1 - m_2}{m_1 - m_3} \times 100\%$$

Where m_1 is the initial weight of the hydrogel, m_2 is the measured weight and m_3 is the final weight of the hydrogel. Data from each specimen was calculated using triplicate measurement.

Biomechanical performance

The compression strength was determined according to our previous studies. Briefly, different hydrogels with a height of 10 mm and a diameter of 18 mm were prepared for the compression test. The displacement rate was set as 5 mm/min. The stress and strain were recorded and calculated until the specimen broke. Data from each sample was calculated using triplicate measurement.

Tissue adhesive mechanical strength

The hydrogels were applied to two pieces of regularly cut porcine heart pericardium and after light curing, the tensile test (5 mm/min) was used to obtain the adhesive mechanical strength. Data from each sample was calculated using triplicate measurement.

Concentration of allicin in hydrogels

We determined the real concentration of allicin in different hydrogel specimens, using UV spectrophotometry according to the reference[1]. Briefly, allicin was able to react with 4-mercaptopyridine (4-MP), which could reduce the absorbance value of 4-MP at 324 nm. Based on this, the amount of allicin loading on hydrogels could be determined. We first plotted the standard concentration curve of allicin, and then the amount of allicin in the solution was measured before and after loading allicin onto hydrogels according to the standard concentration curve. The content of allicin was noted as W_{Before} and W_{After}. The capacity of allicin on hydrogels was calculated by the following eqn:

$$W_{Load} = W_{Before} - W_{After}$$

Antibacterial studies

The antibacterial ability of MCOAC hydrogels was determined by the plate count method, and Staphylococcus aureus and Escherichia coli were used as model bacteria.

The bacteria were first incubated in Nutrient Broth (NB) at 37 ℃ until the exponential growth phase. The bacterial broth was then diluted with saline and a concentration of 1×10^7 colony forming units (CFU)/ml was used for subsequent experiments. Each hydrogel specimen was made into a disk of 1 cm diameter and 4 mm thickness, sterilized and placed in a 12-well plate. 30 μl of the above bacterial suspension and 270 μl of saline were added to the surface of each hydrogel and co-cultivated for 3 h at 37 ℃, the blank well was considered as a control group. Subsequently, the above co-cultured bacterial suspension was diluted about 1000 times and inoculated with 100 μl of this dilution on NB agar plates and incubated at 37 ℃ for 24 h. the reduction rate of bacteria was calculated by counting the number of CFUs on the agar plate. The bacterial reduction rate of hydrogels was calculated as follows:

$$Reduction\ rate\ of\ bacteria\ (\%) = \frac{q_{control} - q_{sample}}{q_{control}} \times 100\%$$

Where q_{sample} and $q_{control}$ were the number of CFUs on the agar plate for the hydrogel sample group and the control group. Data from each sample was calculated using triplicate measurement.

Cytotoxicity assay for chondrocyte

Chondrocyte were cultured in F12 medium which was supplemented with 10% FBS and 1% penicillin-streptomycin. Cells were incubated at 37 ℃ with 5% CO_2. The growth medium was replaced every other day and the passage 3 were used for

cytocompatibility test. All hydrogels were sterilized by γ-rays with an irradiation measurement of 25 KGy before test.

P3 generation of chondrocyte (100 μl, 1×10^5 cells/ml) were slowly dropped on the surface of each specimen in the well of 24-well culture plates. After incubation for 3 h, 500 μl serum-containing medium was added to each well. These 24-well plates were incubated at 37 ℃ with 5% CO2, and the medium was changed every other day. After seeding, the cell-specimens were incubated for 1, 3, 5days. Subsequently, all cell-specimens were transferred to 24-well plates with containing 500 μl of fresh medium and 50 μl of CCK-8 in each well, and incubated for an additional 1 h at 37 ℃. Then, 100 μl of the solution was taken from each well and added to a 96-well plate, and the absorbance was measured at 450 nm using a microplate reader (model 550, BioRad). The percentage of relative growth rate (RGR) was used to express the cytotoxicity and calculated as following equation:

$$RGR(\%) = \frac{OD_1}{OD_0} \times 100\%$$

Where OD_1 is the optical density of cells cultured with different hydrogels, and OD_0 is the optical density of cells cultured in the control group. Experiments were performed in six replicates.

A Calcein/PI Live/Daed Viability/Cytotoxicity Assay Kit was used to study the cell viability of chondrocyte. Cells were seeded on the surface of the samples with a density of 1×10^5 cells/well. After incubation for 3 days, cell were observed and imaged under microscopy (VMF30A).

Chondrocyte morphology observation

After chondrocyte was seeded on hydrogels and continuously incubated for four days, their attachment morphology was observed by SEM. In brief, samples were washed by PBS, and then they were fixed by 4% paraformaldehyde/PBS solution at 4 ℃ for 12 h. Various cell-loaded hydrogel specimens were dehydrated in gradient ethanol (30%, 50%, 70%, 90%, 95%, 98%, and 100%, respectively) at each concentration for 15 min. Finally, cell-loaded samples were critical point-dried and sputter-coated with gold. SEM was employed for the final observation.

To further evaluate the growth and distribution of chondrocyte on different hydrogel specimens, chondrocyte was stained with rhodamine-phalloidin/DAPI and observed using CLSM. The cell-loaded hydrogel samples were prepared as detailed above. after incubating for four days, the cell-loaded samples were washed with PBS

solution several times and fixed by 4% paraformaldehyde/PBS solution for 30 min. Subsequently, the samples were immersed in Triton X-100 for 5 min to improve cell membrane permeability. Then 200 μl of 12 mM rhodamine-phalloidin solution and 1 ml of 5μg/ml DAPI solution were added to stain the cytoplasm and cell nucleus.

Morphology of RAW264.7

To evaluate the growth and distribution of RAW264.7 on different hydrogel specimens, RAW264.7 was stained with rhodamine-phalloidin/DAPI and observed using CLSM. The specific staining method was the same as for chondrocytes.

Cytotoxicity assay for BMSCs

The cytotoxicity of BMSCs on the surface of MCOAC hydrogels was determined using CCK-8. The specific method was the same as for chondrocytes.

Morphology of BMSCs

To evaluate the growth and distribution of BMSCs on different hydrogel specimens, cells were stained with rhodamine-phalloidin/DAPI and observed using CLSM. The specific staining method was the same as for chondrocytes.

Patellar wear and knee joint inflammation

Rabbits kept until the specified time after surgery were over-anesthetized and executed and sampled. Briefly, the patella was removed by carefully dissecting open the knee joint of the rabbit and immediately immersed in 4% paraformaldehyde for fixation. The knee joint was then gently flushed with saline using a 1 ml insulin syringe, and the flush fluid was collected. The fluid was packed in a 1.5 ml sterile centrifuge tube and centrifuged at 1000 r/min for 5 min at 4 ℃. The supernatant was collected and the amount of TNF-α and IL-1β in the supernatant was measured using ELISA kits.

After 24 h of fixation, the patella was gradient dehydrated through ethanol (30%, 50%, 70%, 90%, 95%, 98%, 100%). After critical point drying and gold spraying, the patella surface was observed using SEM.

Synchrotron radiation tomography

To understand the subchondral bone and cartilage regeneration at the defect site after 4 and 12 weeks, the formalin fixed tissues (with defects) were studied by

microtomographic (micro-CT, scanco viva CT80) observations. In brief, the air dried tissue were scanned at a voltage of 85 kV, and a current of 90 μA without any filter. The exposure was set to 500 ms per image with 1000 images captured per complete rotation. The voxel size was fixed as 23 μm. Reconstruction of the 2D and 3D projections was performed using Mimics.

1

Results and discussions

Particle size distribution of DCP

The result of the particle size distribution of DCP was shown in Fig. S1. It could be seen that after ball milling, the diameter of DCP was mostly distributed in 2-5μm. However, there were still a small number of particles with large diameters. This might be due to that ball milling was not able to completely grind the decellularized cartilage and there was a certain degree of agglomeration of DCP, which will increase the diameter of some particles.

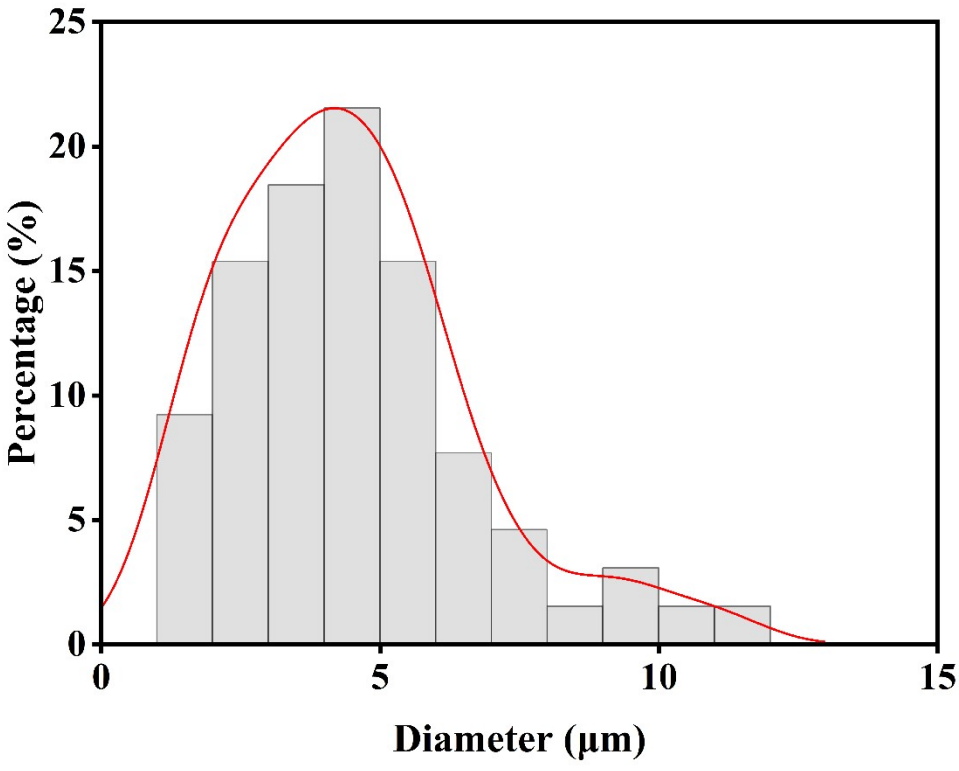

Fig. S1. Particle size distribution of DCP.

SEM for monodisperse DCP

To further characterize the size of DCP, we supplemented the monodisperse SEM images of DCP. As shown in Fig. S2, after ultrasonic dispersion, individual DCP could be clearly observed, and their sizes were about 4-5 μm, which was the same as the result for particle size statistics. The monodisperse DCP images further proved that we obtained smaller sized DCP through low-temperature ball milling.

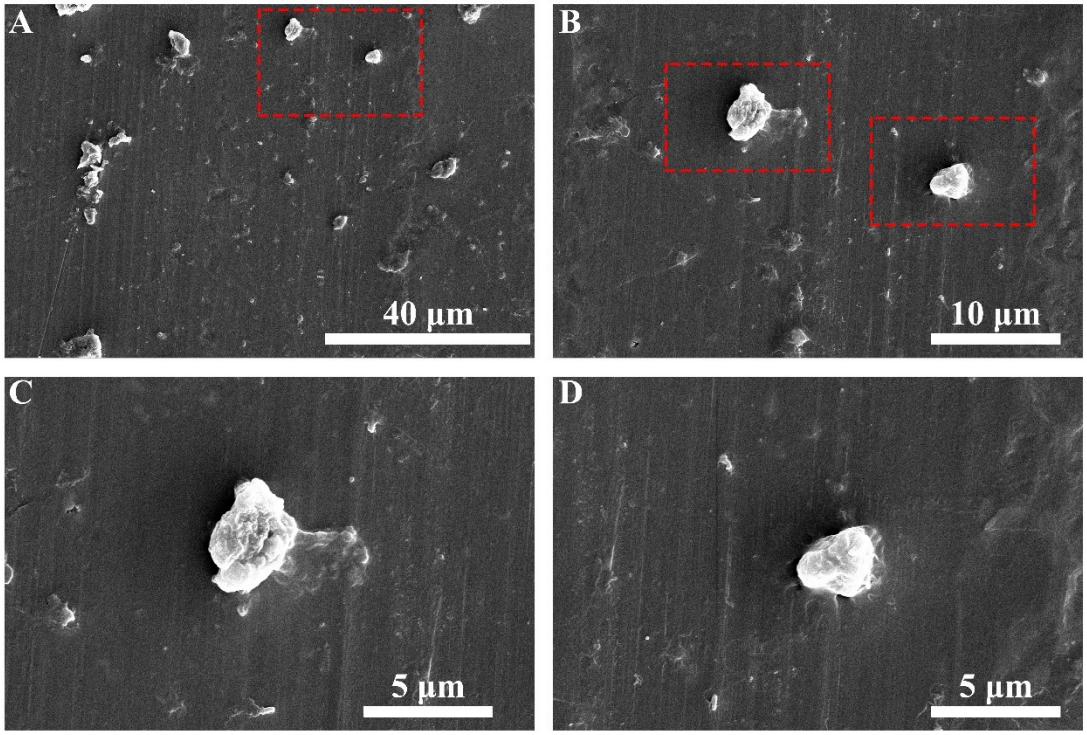

Fig. S2. Monodisperse morphology for DCP. (A): 4000 × SEM image of DCP; (B): 10000 × SEM image of DCP; (C-D): 20000 × SEM image of DCP; Red dashed box shows further zoomed positions.

Distribution of elements for DCP

It could be seen from Figure S3 that DCP contains elements such as carbon, oxygen, sulfur, and calcium. The high content of carbon elements in the figure was due to the high amount of carbon in the conductive adhesive. However, the distribution of these elements was further evidence that the decellularization and ball milling treatment of cartilage did not destroy the compositional composition of the cartilage.

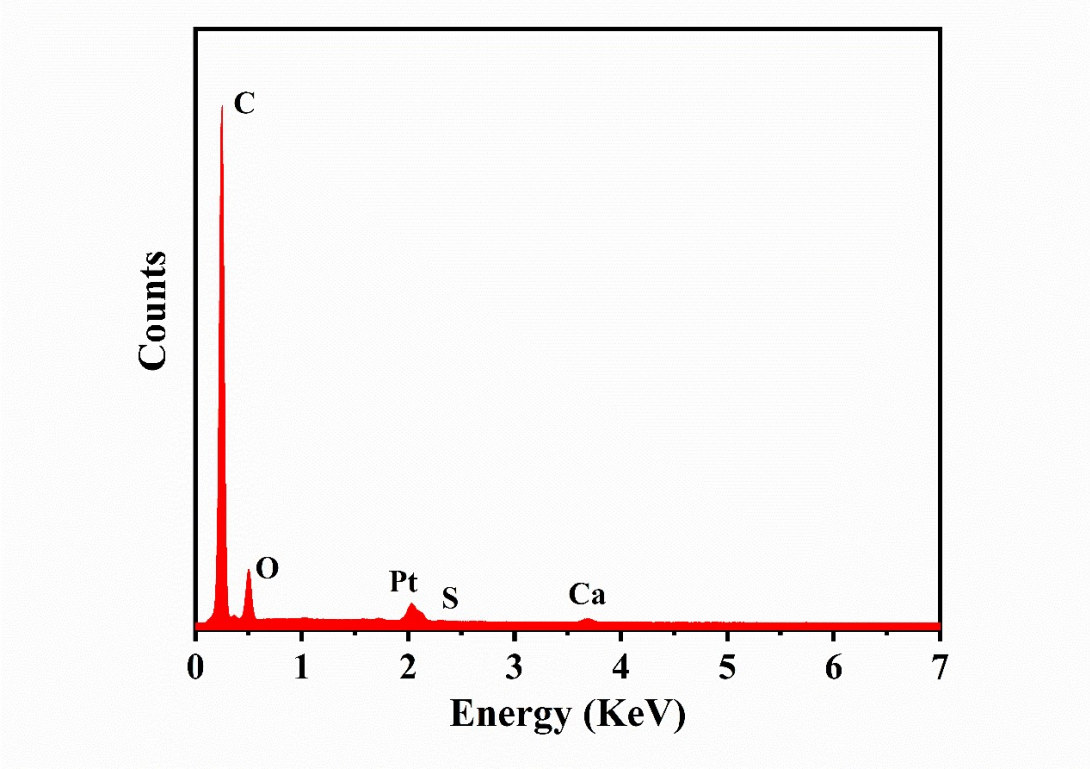

Fig. S3 Element intensity spectrum of DCP.

Degradation and cytocompatibility of DCP

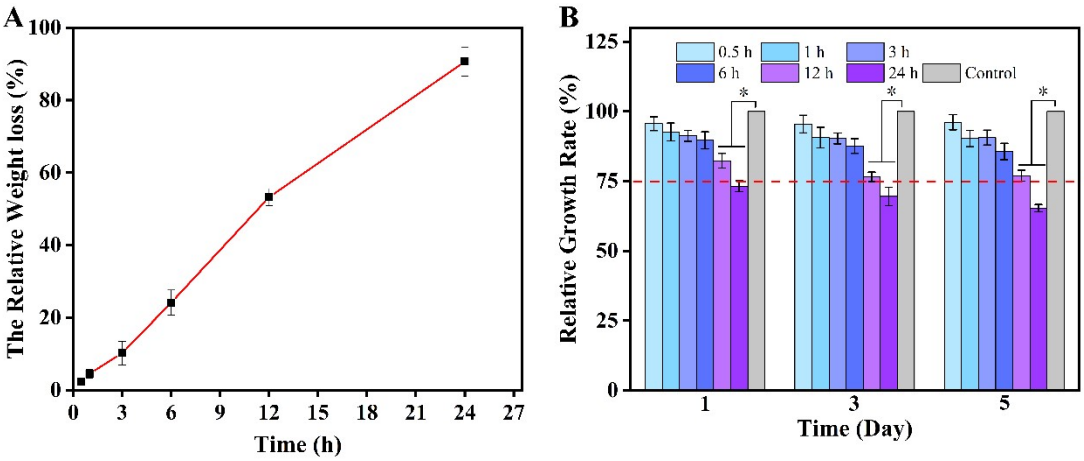

Fig. S4. (A): The degradation ratio of DCP; (B): Cytocompatibility of DCP degradation ingredients at different degradation time points.

It could be seen from the figure that DCP was rapidly degraded in a short period of time under the action of type II collagenase, with a weight loss of 84% at 24 h. This was due to that the main component of DCP was type II collagen, which could be quickly hydrolyzed by collagenase. Immediately following this, we tested the

cytotoxicity of DCP degradation ingredients. As shown in Fig. S4B, the degradation products of DCP during a short degradation time were not very toxic to the cells, but the cytotoxicity of DCP degradation products gradually increased with the prolongation of the degradation time. While the DCP degradation products after 24 h of enzyme action showed strong cytotoxicity at the early stage of cell culture (1 d). This proved that the degradation products of DCP in MCOAC hydrogels produce certain cytotoxicity, which in turn reduces the cytocompatibility of hydrogels.

Crosslinking degree of OLBG and MA-CMCS

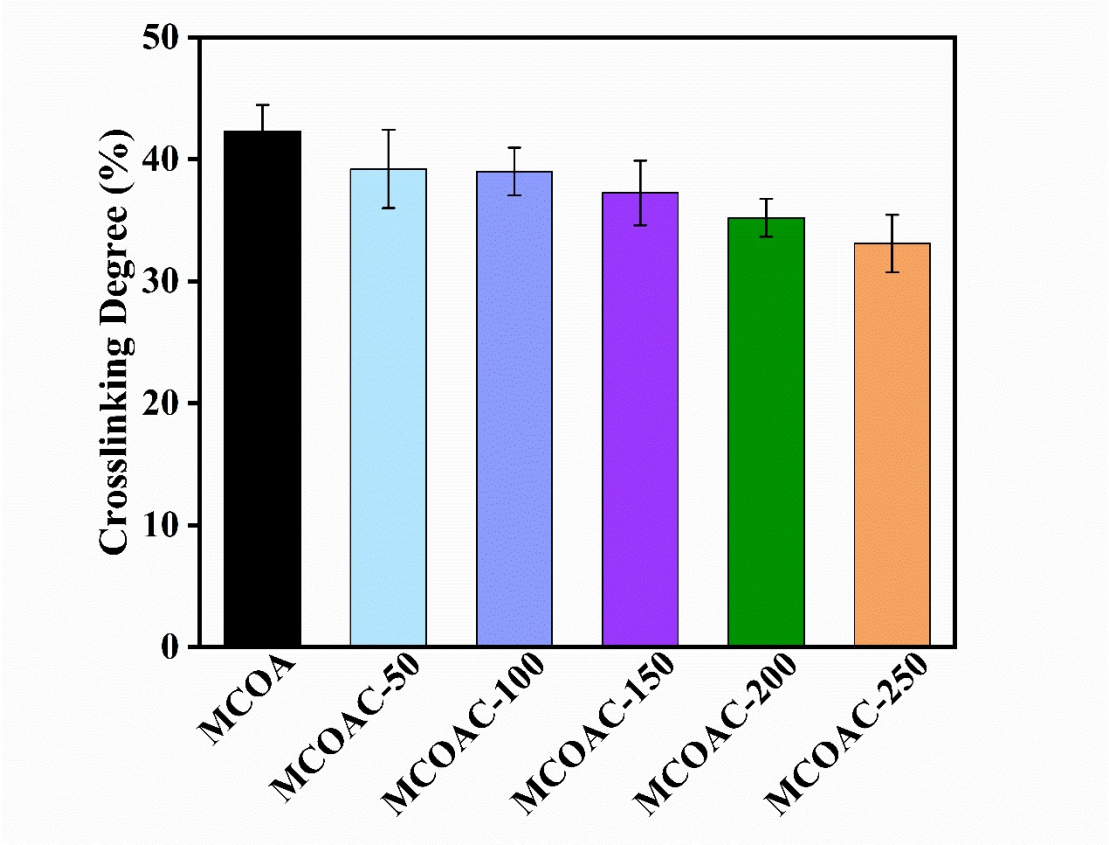

Fig. S5. Crosslinking degree of OLBG and MA-CMCS in different hydrogels.

The results of the crosslinking degree of OLBG and MA-CMCS were shown in the above figure. It could be seen that the crosslinking degree of MCOA hydrogel was only 41.23%, which was because the addition of OLBG in the hydrogel was small and was only capable of reacting with some of the amino groups in MA-CMCS, thus the crosslinking degree was low. It could also be found that, with the increase of DCP, the crosslinking degree of OLBG and MA-CMCS decreased. This was because part of the aldehyde group in OLBG reacted with the amino group in DCP, which in turn reduced

the reaction with MA-CMCS.

Injectability of hydrogels

As shown in Fig. S6, the hydrogel precursor solution could be extruded uniformly from the syringe and form a stable shape. After photocrosslinking, a specific shape hydrogel could be obtained.

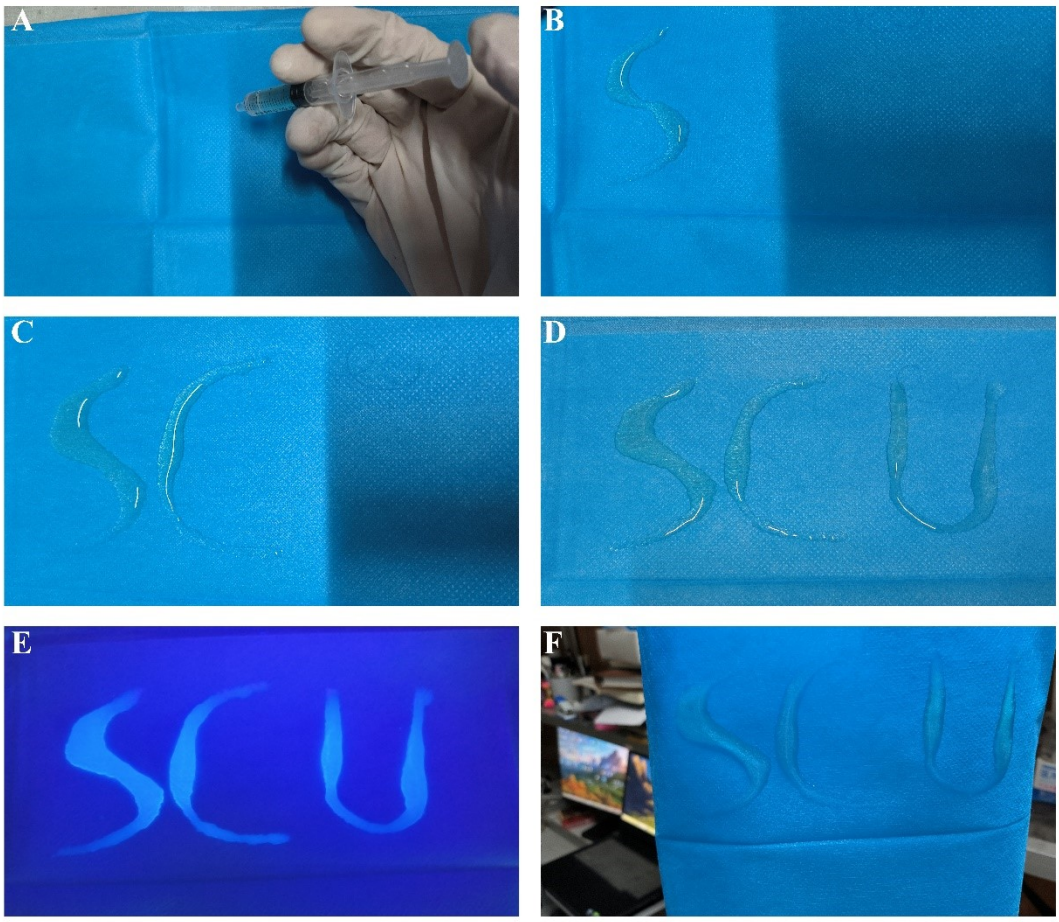

Fig. S6. Injectable properties of hydrogel. (A-D): Injection for hydrogel precursor solution; (E): UV crosslinking for hydrogel; (F): Hydrogel after crosslinking.

Biomechanical performance

The experimental results of compressive mechanical properties of different hydrogels were shown in Fig. S7. It could be seen that, the compression strength of hydrogels showed a slightly increasing trend with the increase of DCP content (19.61 ± 1.41 KPa for MCOAC-150), which may because the uniform distribution of DCP within hydrogels could effectively absorb the compressive stress. However, hydrogels with high DCP concentrations showed early fragmentation in the test (red-circled in

Fig. S7A). This was because high DCP content destroyed the microstructure of hydrogel, leading to a decrease in compressive strength.

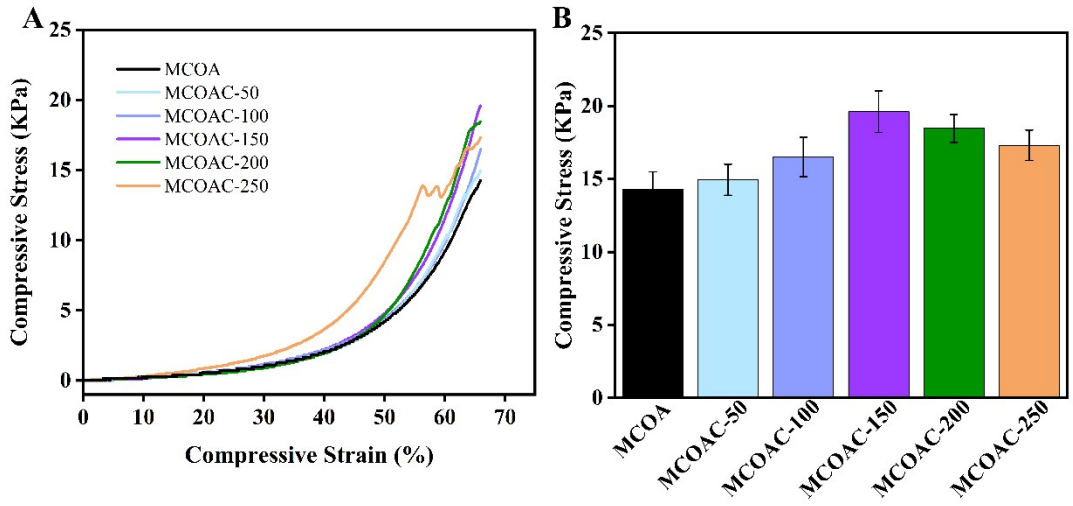

Fig. S7. Compressive test for different hydrogels. (A): Compression curves for different hydrogels; (B): Maximum compressive strength for different hydrogels.

Tissue adhesive mechanical strength

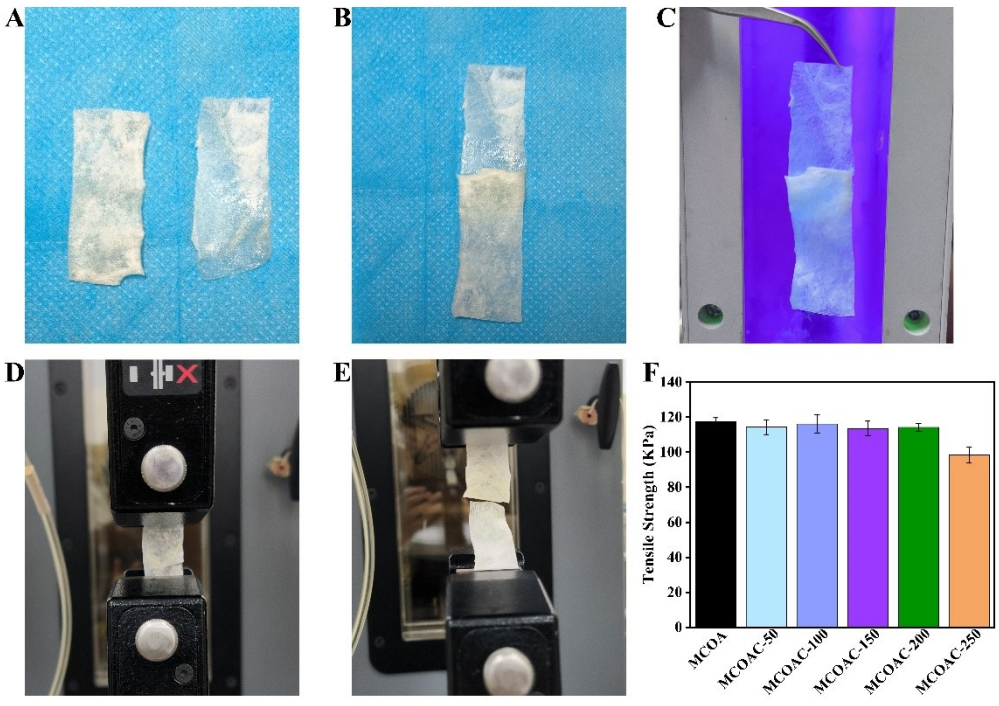

Fig. S8. Tissue adhesive mechanical strength for different hydrogels. (A-C): Schematic diagram of hydrogel adhesion to porcine pericardium; (D-E): Schematic diagram of tensile test; (F): Adhesion strength for different hydrogels.

It could be seen in the figure (Fig. S8) that the hydrogel showed good adhesion ability. Meanwhile, lower concentrations of DCP did not lead to a decrease in the adhesion strength of hydrogel. However, this test was only a preliminary characterization of the adhesion capacity of hydrogel, not representative of the ability of hydrogel to adhere to tissues in real environments (uneven surfaces). Based on your constructive suggestions, we will optimize the adhesion test of our hydrogels in subsequent experiments. Thank you again for your valuable comments.

Concentration of allicin in hydrogels

It could be seen from Fig. S9 that MCOA hydrogel had higher allicin concentrations compared with MCOAC hydrogels, and the concentration of allicin in MCOAC hydrogels gradually decreased with the increase of DCP content. This was probably due to that DCP adsorbed some allicin and prevents it from participating in crosslinking. These adsorbed allicin then escaped from hydrogel under PBS immersion, which ultimately led to a lower allicin content in hydrogel.

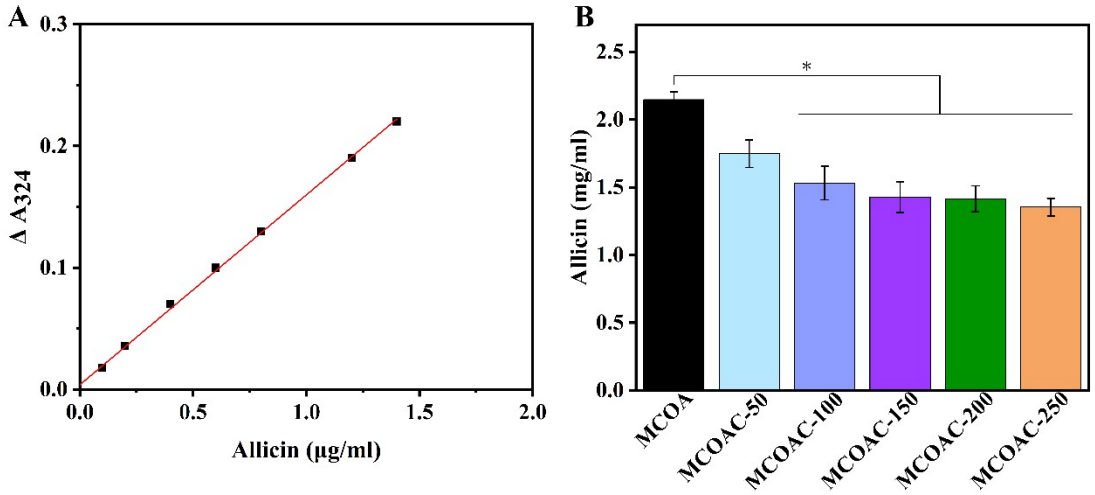

Fig. S9. Allicin concentration in different hydrogels. (A): Allicin content standard curve; (B): Allicin concentration in different hydrogels.

Morphology of chondrocyte

The CLSM images of chondrocytes after co-culture with different hydrogels were shown in Figure S10. It could be seen from the figure that the chondrocyte spreading on the surface of the MCOAC hydrogels was better than that of the MCOA hydrogel. The cytoskeletal structure and cellular microfilaments could be more clearly observed. This further indicates that DCP could effectively improve the chondrocyte

compatibility of the hydrogels.

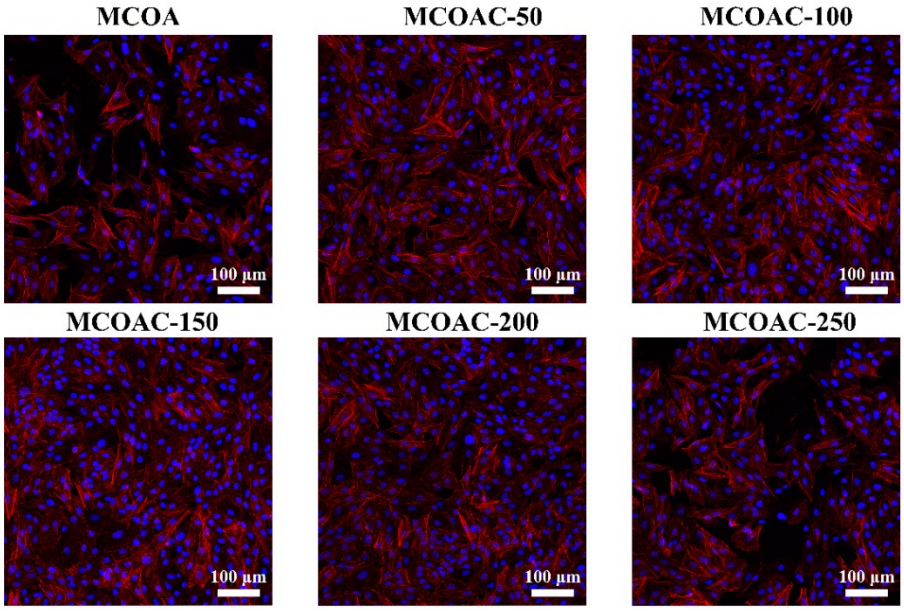

Fig. S10 CLSM images of chondrocyte

Reference

1. I. S. Talia Miron, Guy Feigenblat, Lev Weiner, David Mirelman, Meir Wilchek, and Aharon Rabinkov, *Analytical Biochemistry*, 2001, **307**, 76-83.